Nat. Hazards Earth Syst. Sci. Discuss., 3, 7587–7630, 2015
www.nat-hazards-earth-syst-sci-discuss.net/3/7587/2015/
doi:10.5194/nhessd-3-7587-2015

Natural Hazards and Earth System Sciences
Discussions

Influence of meteorological factors on rockfall occurrence in a middle mountain limestone cliff

J. D'Amato[1], D. Hantz[1], A. Guerin[3], M. Jaboyedoff[3], L. Baillet[1], and A. Mariscal[1,2]

[1]Univ. Grenoble Alpes, ISTerre, 38041 Grenoble, France
[2]IRD, ISTerre, 38041 Grenoble, France
[3]Center for Research on Terrestrial Environment (CRET), Faculty of Geosciences and Environment, University of Lausanne, Unil-Mouline, Geopolis, 1015 Lausanne, Switzerland

Received: 26 November 2015 – Accepted: 28 November 2015 – Published: 21 December 2015

Correspondence to: D. Hantz (didier.hantz@ujf-grenoble.fr)

Published by Copernicus Publications on behalf of the European Geosciences Union.

Abstract

The influence of meteorological conditions on rockfall occurrence has been often highlighted, but its knowledge is still not sufficient due to the lack of exhaustive and precise rockfall data bases. In this study, rockfalls have been detected in a limestone cliff by annual terrestrial laser scanning, and dated by photographic survey during 2.5 years. A near-continuous survey (1 photo each 10 mn) with a wide-angle lens have allowed dating 214 rockfalls larger than 0.1 m^3, and a monthly survey with a telephoto lens, dating 854 rockfalls larger than 0.01 m^3. The analysis of the two data bases shows that the rockfall frequency can be multiplied by a factor as high as 7 during freeze–thaw episodes and 26 when the mean rainfall intensity (since the beginning of the rainfall episode) is higher than 5 mm h^{-1}. Based on these results, a 4-level scale has been proposed for predicting the temporal variations of hazard. The more precise data base and freeze–thaw episode definition make it possible to distinguish different phases in freeze–thaw episodes: negative temperature cooling periods, negative temperature warming periods and thawing periods. It appears that rockfalls occur more frequently during warming and thawing periods than during cooling periods. It can be inferred that rockfalls are caused by thermal ice dilatation rather than by dilatation due to the phase transition. But they may occur only when the ice melt, because the cohesion of the ice–rock interface can be sufficient to hold the rock compartment which has been cut.

1 Introduction

Rockfalls are sudden phenomena, usually non predictable in time but sometimes in space, which can cause human or material damages. The geological and morphological context of a given site affects the rockfall activity, but rockfalls can be triggered by external factors (Cruden and Varnes, 1996) such as meteorological factors (see references in Table 2), earthquakes (Kobayashi et al., 1990; Malamud et al., 2004; Yin et al., 2009), volcanic eruptions (Hale et al., 2009; DeRoin and McNutt, 2012), sea

waves (Rosser et al., 2005), human activity. Several studies have highlighted the influence of these different triggering factors, but triggering mechanisms are still not well understood and quantified, especially considering the influence of meteorological factors. We need to better understand the triggering mechanisms of rockfalls, to enhance the quantitative assessment of rockfall hazard and the prediction of high hazard periods according to the meteorological forecast. Moreover, this is an important step to assess the influence of climate change on rockfall hazard (Huggel, 2012; Sass and Oberlechner, 2012).

Rockfalls are a result of a long geological process (tectonic, weathering...) (Viles, 2013), but the fall is sudden. The more asked question is why does the rock fall at a given time? Behind this, the real question is what makes it fall (what factors?), and how (what mechanisms?). Considering a meteorological factor, several physical mechanisms can be involved, which can act for rockfalls initiated by a slide or a topple (Luckman, 1976). In Table 1, we propose some physical processes associated to different meteorological events, which can trigger a rockfall, and the associated relevant meteorological parameters.

Most of works concerning these factors are based either on a single event study (Yamagishi, 2000; Wei et al., 2014), or on a rockfall inventory. Some examples of studies based on a rockfall inventory are given in Table 2. They show the influence of meteorological factors, but it is not possible to conclude on a dominating triggering factor, partly because these studies present several disparities concerning:

- the geological and climatic context (from coastal to high mountain);
- the size and completeness of the rockfall inventory (from 10 to almost 1000 events);
- the precision of dating (from day to year);
- the precision of meteorological data, in time and space (frequency of the measures, distance to the site);

- the method of analysis, e.g. thawing periods not precisely defined.

This study deals with a quasi-exhaustive rockfall inventory, obtained by Terrestrial Laser Scanner (TLS), now classically used for rockfall survey (see reviews in Jaboyedoff et al., 2012; Abellan et al., 2014), combined with a photographic survey. The study site is a cliff with homogenous lithology, avoiding geological, geomorphological, and climatic bias. We use 2 level of dating precision. Besides, we defined new precise meteorological parameters in order to better evaluate triggering processes related to meteorological factors, especially considering freeze and thaw which are not often clearly defined in the literature.

2 Study site

The Mont Saint Eynard (MSE) is located north east of Grenoble, Isère, French Alps (Fig. 1). It is a long double cliff, making up the western border of the Isère Valley and the oriental edge of the Chartreuse Massif. The lower cliff is 240 m high, separated from the 120 m high upper cliff by a ledge covered with forest. The upper cliff consists of massive limestone (bed thickness > 1 m) of the Tithonian stage. The lower cliff consists of fractured thin bedded (10–50 cm) limestone, of the Sequanian stage. The bedding planes dip inside the cliff. This anaclinal configuration, completed by subvertical fractures, produces overhanging compartments falling mainly by toppling.

This SW–NE trending cliff belongs to the eastern side of the Sappey syncline, which dips north in the direction N10. Two subvertical dextral faults cut the cliff (Gidon, 1990), with a direction of about N60–70. Note that the global direction of the Saint Eynard cliff (N45) is different from the syncline axis (N10).

A 750 m long zone of interest (photograph on Fig. 1) has been yearly surveyed by TLS since 2009 (Guerin et al., 2014). This study focuses on the MSE lower cliff for several reasons:

- high rockfall activity compared to the upper cliff (Fig. 1);

– large volume range: from 0.001 m^3 to more than 1000 m^3 (exceptional event);

– lithological homogeneity;

– entire cliff faces south: homogenous sun exposition.

The climate of the Grenoble town is characterized by a mean annual precipitation of 934 mm, a mean minimal temperature of 6 °C and a mean maximal temperature of 16 °C (measures from 1981 to 2010 at an elevation of 200 m). At the elevation of the MSE lower cliff (800 to 1050 m), the precipitation is higher: the gradient is of 28 mm yr^{-1} per 100 m in this zone (Douguédroit and Saintignon, 1984). Also, the mean annual temperature is lower than in Grenoble: a temperature gradient of 0.6 °C per 100 m is usually considered, but our temperature measures on the cliff show a lower gradient of 0.3 °C per 100 m, due to the southern exposition of the cliff and the morphology of the Isère valley (Jail, 1966a).

3 Methodology

3.1 Rockfall detection by TLS

Rockfall detection is carried out by a diachronic comparison of point clouds of the cliff acquired in November 2012 and April 2015, by terrestrial laser scanning. A laser scanner Optech Ilris-LR has been used (Optech, 2015). Four acquisitions were carried out at the dates: 16 November 2012, 26 November 2013, 15 July 2014, and 22 April 2015.

The raw point clouds are cleaned, in order to remove vegetation noise and keep only the rock surface (Abellan et al., 2014). They are georeferenced using a georeferenced 1 m spacing DEM (from the IGN, French national institute of geography) of the site. A mesh is built with the point cloud acquired the year Y. For detection of rockfalls, this mesh is registered with the point cloud of the previous year, $Y - 1$, using the software 3DReshaper©. The positive deviations higher than 10 cm are considered as rockfalls.

The point clouds defining a fallen compartment are meshed, allowing to calculate the volume of the compartment and to get dimensions and gravity center. The method is described with more details in Guerin et al. (2014). It allows exhaustive detection of rockfalls larger than 0.05 m^3.

3.2 Rockfall dating by photographic survey

A photographic survey from 1 km of the cliff permits to date the occurred rockfalls. It consists of high resolution photographs taken every several weeks (periodic survey) and lower resolution photographs taken every 10 min (continuous survey, with an autonomous snapping system). Technical information is given in the Table 3.

854 rockfalls have been detected between 16 November 2012 and 22 April 2015 (887 days). Each of these rockfall has been dated by comparing high-resolution photographs, taken every 2 to 11 weeks (37 days in average) They constitute the database 1 (DB1). Rockfalls were considered only when there were evident clues of the fall on the photographs: visible scar, obvious change in color, shadow, or relief (Chanut et al., 2011).

From 1 February 2013 to 22 April 2015, this periodic high resolution photographic survey has been completed by a low resolution quasi-continuous survey (one photo every 10 mn). 214 rockfalls have thus been dated more precisely in intervals of 10 min to 25 days. They constitute the database 2 (DB2). Only 25 % of the DB1 events were dated precisely, mainly due to the photographic resolution: the smallest rockfalls are hardly identified on low resolution photographs. Schematically, one pixel of photographs from the continuous survey corresponds to a surface area of 0.04 m^2. It is thus not surprising that the smallest rockfalls of DB2 have volumes of 0.04 m^3, while the smallest ones in DB1 have volume of 0.002 m^3. The volume distributions for the 2 databases are given on Fig. 2. Obviously, rockfalls occurring during the night can not be dated with a precision better than about 12 h. Moreover the dating uncertainty may be higher due to the meteorological conditions: the entire cliff face or part of it can be hidden (clouds, fog, snow). On sunny days, strong shadows can also “mask” the com-

partment location for a long time. The dating uncertainty can also be due to technical issues: the snapping system sometimes stopped during several days. It ensues that only 70 % of DB2 rockfalls (144 events) have been dated in periods of 10 min to 20 h.

3.3 Meteorological data acquisition and treatment

3.3.1 Meteorological data

The meteorological data come from weather stations of Météo France network around the cliff, and since February 2014, from temperature sensors which have been placed on the upper cliff (1290 m a.s.l.) and inside the rock.

Rainfall data are given by a rain gauge located 900 m from the cliff face, with an hourly frequency. The raw data correspond to the number of gauge runnel (0.2 mm) swaying per hour.

The valley temperature is measured in a station located around 2 km from the cliff face at an elevation of 245 m. The temperature is measured (each 10 min) on the upper cliff (1290 m elevation) only since February 2014, with temperature sensors in open rock joints (2–4 cm opening) at a depth of about 10 cm, and in two sealed boreholes at depths of 20 and 50 cm. Because we study the action of the ice in rock joints, we have considered the air temperature in the open joints (almost always in the shade). To have a constant method to estimate this temperature at the elevation of the lower cliff, the mean temperature gradient has been determined between the valley temperature and the upper cliff temperature, over a period from February 2014 to April 2015. The value obtained (0.003 °C m^{-1}) is lower than the average temperature gradient usually known (0.006 °C m^{-1}), due to the south exposition of the slope and the topographic setting, but close to the value obtained by Jail (1966a, b) for the MSE slope. The lower cliff temperature T has been estimated from the temperature gradient and the valley temperature, using the Eq. (1):

$$T = T_{\mathrm{m}} - 0.003 \cdot (Z - Z_{\mathrm{m}}) \quad (1)$$

with T_{m} the temperature measured in the valley, Z the mean elevation of the rockfall sources in the lower cliff (900 m), Z_{m} the elevation of the measuring station.

3.3.2 Definition of rainfall episodes

Rainfall episodes have been defined in order to better estimate the influence of rain. The beginning of a rainfall episode is associated to the first record of the rain gauge following a given period without rain (Bertrand-Krajewski, 2007). This first record occurs when the runnel capacity (0.2 mm) is reached. It follows that, beside the uncertainty due to the recording frequency, there is a delay between the true beginning of a rainfall and the first record. Moreover, rainfalls smaller than 0.2 mm are not detected.

A rainfall episode begins when it begins to rain after a given length of time without rain (Bertrand-Krajewski, 2007). This length has been chosen so that the rainfall episodes are independent. We have considered that 2 rainfall episodes are independent if the effects of the first episode stop before the second episode begins (Fig. 3). The direct influence of rain starts when falling on the cliff, but we have to take into account water which falls on the forested ledge, and goes through soil and rock to reach the cliff surface and flow on it. The period of influence has been chosen from field observation of water seepage on the cliff (photographs). We have assumed that after around 24 h, the rainwater has entirely flown from the cliff (Fig. 3).

With this definition, 148 rainfall episodes during 2.4 years have been determined. The distribution of the duration of these episodes is given in Fig. 4. The total duration of the rainfall episodes represents 24 % of the observation period.

The data do not distinguish between rainfall and snow, all considered as precipitations (Bertrand-Krajewski, 2007). As a first approximation, we can assume that snow occurs when temperature is negative with precipitation. This concerns less than 1 % of the precipitation time. So, snow falls were not considered.

3.3.3 Definition of freeze–thaw episodes

The influence of ice on rockfall occurrence can be explained by the pressure it exerts in rock discontinuities (Davidson and Nye, 1985; Walder and Hallet, 1985; Bost, 2008), either when the ice forms in a confined environment (joints, cracks or pores), or when it dilates during heating episodes. But it has also been observed that rockfalls frequently occur after a freezing period, when the temperature is positive (Matsuoka and Sakai, 1999). In order to investigate these processes, the freeze–thaw episodes have been divided in three types of periods: cooling periods (when the negative temperature decreases), warming periods (when temperature increases but remains negative) and thawing periods (when temperature is positive and ice melts).

Our observations show that ice is produced where water seeps slowly on crack walls and when the temperature of the rock surface is negative. This accretion process can go on for several days because the temperature inside the rock mass remains positive, allowing water seepage and migration to continue (Tharp, 1987; Murton et al., 2006; Hallet, 2006). Assuming that water seepage in the rock mass is constant, it is considered that the ice production is reflected by the Freezing Potential (FP), which has been used by Matsuoka (1994) for studying the freeze depth and by Montagnat et al. (2010) for studying the formation of ice columns. For a freeze–thaw episode beginning at t_0, FP is defined by Eq. (2):

$$\text{If } \int_{t0}^{t} (T_\mathrm{f} - T(t))\mathrm{d}t < 0, \quad \text{then FP} = 0$$

$$\text{If } \int_{t0}^{t} (T_\mathrm{f} - T(t))\mathrm{d}t > 0, \quad \text{then FP} = \int_{t0}^{t} (T_\mathrm{f} - T(t))\mathrm{d}t \tag{2}$$

with T_f the freezing point of water (0 °C) and $T(t)$ the temperature at the time t. As a first approximation, we consider that the ice has entirely melted when FP return to

zero. This point defines the end of the freeze–thaw episode (Fig. 5). A freeze–thaw episode begins when the temperature becomes negative and no freeze–thaw episode is in progress (there is no more ice in the rock mass).

A freezing period begins when the temperature becomes negative ($t = t_0$). The FP becomes positive. It ends when the temperature becomes positive again. At this point the FP starts to decrease. A freezing period may include several cooling and warming periods. During cooling periods, the thermal contraction of existing ice tends to decrease the ice pressure. On the other hand, ice expansion occurs during negative warming periods and is proportional to the temperature increase. Ice melting occurs when the temperature becomes positive (thawing period). A thawing period ends either when the temperature becomes negative again (new freeze period), or when FP reaches 0 (no more ice). Note that a freeze–thaw episode may include several freezing and thawing periods. Figure 4 show the distribution of the duration of freezing and thawing periods.

4 Results

4.1 Results on the DB1

The rockfall frequency (h^{-1}) is given for each observation period in Fig. 7. As the dating periods have different lengths, we have not considered the absolute rainfall and freeze–thaw durations, but the time proportion of rainfall and freeze–thaw (respectively Rrd and Rftd) in each dating period. It was calculated by adding the durations of all the rainfall or freeze–thaw periods occurring during a dating period, and dividing the total rainfall or freeze–thaw duration by the length of the dating period (Fig. 6). In the same way, rainfall and freeze–thaw amount ratios (respectively Rra and Rfta) were determined for each dating period by adding all the rainfall amounts or the amplitudes of the FP variations (positive and negative), and dividing the sum by the length of the dating

period (Fig. 6). Using these ratios, the relation between the rockfall frequency and the rainfall or freeze–thaw can be analyzed in Fig. 7.

A first approach allows to visually highlight the influence of some factors. It can be seen that the 7 periods with the highest proportions of freeze–thaw, in duration or amount, give the highest rockfall frequencies. It indicates a strong influence of freeze–thaw on rockfall frequency. However, the influence of rainfall is not so clear. One can observe a factor 10 between the highest and the lowest rockfall frequencies, which occur in periods with few rain.

In order to better quantify the relative influence of these factors, we used a multiple linear regression (Rakotomalala, 2015). It consists of explaining the rockfall frequency with rainfall and freeze–thaw duration ratios or amount ratios. The results are summarized in the Table 4.

The test of the multiple regression, using a Fischer Test, is significant: $F(\text{duration}) = 9.45$ and $F(\text{amount}) = 9.71$, in comparison with $F(0.05;2;20) = 3.49$ at the 0.05 significance level, 2° of freedom, and around 20 observations (here 24). We can then consider that the determination coefficient for the multiple regression R^2, close to 0.5, is also significant. It means that around 50 % of the variability of rockfall frequency can be explained by the variability of rainfall and freeze–thaw duration or amount. The standardized regression coefficients help to estimate the "weight" of each variable on the variability of rockfall frequency. They are given in the Table 4. We can see that the contribution of freeze–thaw (Rftd_{st} and Rfta_{st}) to explain the variability of the rockfall frequency is 5 to 7 times higher than those of rainfall.

Based on a Student test, the influence of freeze–thaw (duration ratio or amount ratio) is significant at the 0.05 significance level, but the hypothesis of no influence of the rain (H_0) can not be rejected. This clearly shows that freeze–thaw influence is more important than rain influence. It confirms visual observations of Fig. 7. These results are consistent with Frayssines and Hantz (2006) who showed that freeze–thaw had a major influence on big historical rockfalls occurred in subalpine limestone cliffs.

As we try to distinguish different potential triggering mechanisms in freeze–thaw cycle (Fig. 4), we determine the duration ratios of ice production (Ripd), negative warming (Rnwd), and thawing (Rtd), and also the amount ratios (Ripa, Rnwa, Rta) (Fig. 6). A multiple linear regression cannot be correctly performed on these type of data because of their collinearity (Rakotomalala, 2015): as a matter of fact, ice production, negative warming and thawing are not independent from each other. We performed the multiple regression on couples formed by each of these parameters with rain (r), in order to determine the parameter having the strongest influence on rockfall frequency. The highest determination coefficient and the lowest Akaike criterion (AIC) (Rakotomalala, 2015) were used to determine the best couple. For both duration and amount ratios, thawing showed the best regression and correlation coefficients, and the lowest AIC. R^2 for the regression is again close to 0.5 (Table 4).

Considering the standardized regression coefficient, thawing shows a clear influence on rockfall frequency, with a contribution on rockfall frequency more than 7 times higher than rainfall. Again, the hypothesis of no rain influence (H_0) can not be rejected for the rain duration and amount, using a Student test. It can be noted that for all the multiple regressions, the constant of the regression represents the rockfall frequency for periods without either rainfall or freeze–thaw. Its value is around $0.021\,\text{h}^{-1}$. It can not be estimated directly because there is no period without freeze–thaw or rainfall.

From this value, one can estimate for the observation periods including freeze–thaw episodes, the number of rockfalls which occur when there is no freeze–thaw, and then the number of those which occurs during freeze–thaw (neglecting the rockfalls due to rain, because they are much less frequent and precipitation is snow during freezing periods). An estimate of the rockfall frequency during freeze–thaw episodes can then be obtained by dividing the number of rockfalls during freeze–thaw by the effective duration of freeze–thaw. A value of $0.147\,\text{rockfalls}\,\text{h}^{-1}$ is obtained, which is 7 times higher than without freeze–thaw or rainfall. In the same way, one can obtain an estimate of the rockfall frequency during rainfall episodes by considering only the periods without freeze–thaw. In this case, a simple regression can be carried out, giving

a constant of $0.012\,h^{-1}$ (Fig. 8). However, the determination coefficient is low. A value of $0.054\,rockfalls\,h^{-1}$ is obtained for the rockfall frequency during rainfall, which is 4.5 higher than without rainfall. However, one must remark that this value is obtained from a poor quality regression and that the hypothesis of no rainfall influence can not be rejected.

4.2 Results on the DB2

Out of the 214 rockfalls forming DB2, we have studied 144 rockfalls, whose date is known with an uncertainty lower than 20 h. This choice induces a bias because the rockfalls occurring during freeze–thaw periods are dated with a higher uncertainty (associated with snow cover, ice cover or fog, which disturb the identification of scars on the photographs). It ensues that the rockfall frequency during freeze–thaw periods is underestimated and then DB2 is less relevant than DB1 for comparing the influences of rainfall and freeze–thaw. But thanks to its higher dating precision, it allows studying more precisely the influence of the different processes occurring during a freeze–thaw episode, and the period of influence of a rainfall episode.

Different meteorological conditions have been studied. Two types of frequency were considered (Table 5). The "certain" frequencies are obtained by considering only the rockfalls whose the dating interval is entirely included in an episode of freeze–thaw or rainfall, in a period of negative cooling, negative warming or thawing (Fig. 4), within different periods following a rainfall episode (0–24, 24–48 or 48–72 h) or in a period with none of these conditions. The "statistical" frequencies are obtained by considering also the rockfalls whose the dating interval belongs to several meteorological periods. For these rockfalls, the middle of the dating interval has been considered.

It appears in Table 5 that the rockfall frequency (certain or statistical) during freeze–thaw episodes or rainfall episodes is clearly higher than in periods with no particular meteorological condition. The frequency during rainfall episodes is even higher than during freeze–thaw episodes, but the last one is underestimated in DB2. Moreover it

appears that the statistical frequencies within the days following a rainfall episode are not significantly higher than during periods with no particular meteorological condition (they are even lower when considering the certain frequencies).

It appears that during freeze–thaw episodes, rockfalls can occur during the three different types of period, but the rockfall frequency during negative cooling periods is not significantly higher than without any meteorological event (higher for the statistical frequencies, but lower for the certain frequencies). On the other hand, it is clearly higher during negative warming periods and mostly during thawing periods (by a factor 1.2 for the statistical frequencies, and 1.7 for the certain frequencies). As the rockfall frequency is already 7 times higher during freeze-thaw episodes than without freeze-thaw (result from DB 1), it can be derived that it is about ten times higher during thawing periods.

The amount and the duration of rainfall since the beginning of the rainfall episode until the compartment falls have been determined for each rockfall occurred in a rainfall episode. Rockfalls were supposed to occur at the middle of the uncertainty interval. Instantaneous (hourly) rainfall intensity and mean rainfall intensity (since the beginning of the episode) have also been determined. For each class of rainfall amount, duration and intensity, rockfall frequency has been determined (Fig. 9).

Considering the rainfall amount, the class]30,40] mm shows the highest frequency. Remarkably the frequency decreases for the class]40,80]. Considering the rainfall duration, the rockfall frequency is the highest for durations shorter than 25 h. It appears that most rockfalls occur during the first 25 h of a rainfall episode. Remarkably, rainfall durations longer than 50 h do not trigger more rockfalls than no rain. Considering the rainfall intensity, surprisingly the frequency is the highest for the lowest hourly intensity class. It appears that one hour of high intensity rain is not sufficient to trigger rockfalls. However the mean rainfall intensity appears to be a very discriminant parameter because the rockfall frequency becomes very high when this parameter exceeds $5\,mm\,h^{-1}$.

The FP when the rockfall occurred has been determined for each rockfall occurred in a freeze–thaw episode. Freezing periods (assumed to be ice production periods) and thawing periods have been distinguished (Fig. 10).

We can note that rockfall frequency is slightly higher for low FP (between 0 and 100 °C h) when considering the freezing periods, but it is much higher for high FP (400 to 800 °C h) when considering the thawing periods. This suggests that rockfalls occurring during thawing are the most frequent at the beginning of thawing (when the FP is still high) and after a long or intense freezing period. Note that these results are drawn from only 25 rockfalls occurred during freeze–thaw episodes.

No correlation has been observed between the rockfall frequency and the daily thermal amplitude, the maximal or the minimal daily temperature.

5 Discussion

5.1 Analysis of freeze–thaw influence

The global influence of freeze–thaw has been analysed from DB1, because DB2 underestimates this influence. Considering the DB1, it appears that the rockfall frequency is about 7 times higher during freeze–thaw episodes than without freeze–thaw. To be of practical use in terms of rockfall hazard assessment (Hantz, 2011), the rockfall frequency must be associated to the minimal rockfall volume for which the detection is exhaustive and to the surveyed cliff area. For rockfall volumes larger than 0.05 m^3 and for a cliff area of 129 646 m^2, the rockfall frequency during freeze–thaw episodes has been estimated to 0.065 rockfalls h^{-1}.

The DB 2 allows to compare the influence of different types of period during a freeze–thaw episode (Table 5). During freezing periods (negative temperature), our results show that rockfalls occur rather during warming periods than during cooling periods. This result can be surprising because it is often assumed that the ice influence is due to the pressure exerted by ice during the phase transition (Davidson and Nye, 1985; Bost,

2008). In laboratory, Bost (2008) has measured an ice pressure of several MPa when water freezes in an artificial crack in a limestone block. This pressure decreases with time due to the viscous behavior of ice, but it increases again when the temperature increases, due to the thermal ice dilatation. It is noteworthy that this test was carried out with a crack which is initially full of water. However, the authors think that this initial condition does not reflect what really happens in the MSE cliff. It appears from field observation that ice forms by an accretion process due to freezing of water drops slowly seeping on rock or ice surface in non-confined environment (Fig. 11). Note that it is different from that which occurs in permafrost where ice segregation is mainly invoked (Matsuoka, 2001; Dash et al., 2006; Murton et al., 2006). D'Amato (2015) has carried out laboratory tests with different processes of ice formation in artificial cracks or holes in a limestone block. It appears that no pressure is exerted by ice when water is poured progressively in the discontinuity. This result explains why the rockfall frequency is not significantly higher during negative cooling than without meteorological factor. However, negative cooling induces rock contraction, which can result in crack propagation (shrinkage). During negative warming, a crack can propagate due to the expansion of ice, creating an unstable situation. But the rockfall resulting does not necessarily occur immediately because the cohesion or tensile strength of the ice–rock interface (Fiorio et al., 2002) may be sufficient to maintain the rock compartment until the ice has melt. Then rockfalls due to ice thermal expansion may be delayed and occur during the thawing period. However Davies et al. (2000) and Gunzel (2008, 2012) have shown that the shear strength of ice filled discontinuities begins decreasing when the temperature reaches −5 °C. On the other hand, when a thawing period begins, the ice begins melting at the ice–air interface, but not immediately at the ice–rock interface, and the thermal expansion continues for some time. It follows that the frequency of rockfalls resulting from thermal ice expansion is probably underestimated.

The direct influence of thawing is associated to the production of water (from ice or snow melting), which can acts as rainwater.

Several authors have described a correlation between rockfalls and freeze–thaw, using the occurrence of a freeze–thaw cycle (Douglas, 1980; Frayssines and Hantz, 2006; Mateos et al., 2012; Letortu et al., 2012) or the daily minimum temperature (Delonca et al., 2014). From the data of Frayssines and Hantz (2006), which concerns rockfalls in limestone cliffs of the French Subalpine Ranges with volumes between 10 and 10^5 m^3, one can derive that the rockfall frequency is 2.4 times higher the days with freeze–thaw than the days without freeze–thaw (and 1.7 times the mean frequency). Delonca et al. (2014) has determined the rockfall frequency for rock cliffs in magmatic rocks (Auvergne, France) and rockfall volumes between 2 and 6000 m^3. The daily rockfall frequency two days after a strong freezing ($-20\,^{\circ}C < T < -10\,^{\circ}C$) is 3.9 times higher than the frequency without freezing (3.4 times the mean frequency). These influence factors should be smaller if one considers the frequency two days after a freezing day ($T < 0\,^{\circ}C$) but they are not given by Delonca et al. (2014). The influence factors obtained by Frayssines and Hantz (2006) and Delonca et al. (2014) are smaller than the influence factors we derived from DB1, which are of 7 (and 3.7) (Table 6). This can be explained by different rock mass characteristics or/and the different rockfall volume ranges. It would be not surprising that the influence of air temperature would decrease when the volume (and the depth) of the rockfalls increases.

The overall influence of freeze–thaw on rockfalls appears to be clearly recognized, but the influences of the different phases of freeze–thaw are not well known. In Alpine high mountain, Francou (1982) has observed that the rockfall activity in a north-facing wall is maximal in spring when the number of freeze–thaw cycles is maximal, and minimal in winter when the temperature is rarely positive. Sanderson et al. (1986) have shown that the rockfall activity (volume < 1000 m^3) in Norwegian mountains is maximal in early spring when the temperature increases and lower in winter when the temperature is the lowest. Matsuoka and Sakai (1999) has observed the maximal rockfall activity in the Hosozawa cirque (Japanese high mountain) 5–15 days after the melt out of the cirque wall, which represents the delay for thaw penetration to a depth of about 1 m. It appears from these results that the temperature increase causes more rockfalls

than freezing, which is consistent with our results. By using the freezing potential, our study suggests a quantitative method to estimate the duration of thawing and then of the most active period for rockfalls.

At a multi-year scale, several authors have observed that permafrost thawing due to climate change, increases the rockfall frequency in high mountain cliffs, especially during extremely warm summers as in 2003 (Ravanel, 2010; Huggel et al., 2012). From these observations, it is also difficult to identify the processes which have caused the rockfalls.

5.2 Analysis of rainfall influence

The influence of rainfall on rockfall occurrence has not been clearly established from DB1 but the analysis of DB2 has shown that rainfall frequency during rainfall episodes is 2.5–3 times higher than without meteorological event (Table 5). But this influence factor is higher at the beginning of a rainfall episode (Fig. 7): it amounts to 7 in the first 25 h and then decreases to about 1 after 50 h. Considering the mean intensity since the beginning of the episode, the influence factor amounts to 27 if the intensity is higher than 5 mm h^{-1}. Considering the rainfall amount, it amounts to 7.5 if the rainfall amount is between 30 and 40 mm.

The influence of rainfall has been also shown by several authors (Chau et al., 2003; Mateos et al., 2012; Delonca et al., 2014). From a data base with a daily precision, Delonca et al. (2014) determined rockfall frequency for different rainfall conditions and for 2 transportation routes in Burgundy and La Reunion (France), with respectively limestone and volcanic rocks. They found that the more influencing parameters are respectively the rainfall fallen in a 3-day or 2-day interval including the day of the rockfall. It means that the corresponding rainfall periods are statistically 2 days or 1 day long. At the MSE, we found an influence of the rain fallen in rainfall episodes whose length varies between 15 and 205 h (Fig. 5). Considering rainfall episodes, 75 % of rainfall episodes have a duration between 0 and 50 h, which correspond to 1 to 2 days with rainfall, as also shown in Delonca et al. (2014).

From the results of Delonca et al. (2014) for the limestone cliffs, it can be derived that the mean annual rockfall frequency is multiplied by 6 when the rainfall intensity of the 2-day rainfall period preceding the rockfalls is between 1.5 and 3 mm h^{-1} (maximal value observed). For the volcanic cliffs, the mean annual rockfall frequency is multiplied by 8 when the rainfall intensity of the 2-day rainfall period preceding the rockfalls is between 5 and 8 mm h^{-1}, and this influence factor decreases for higher rainfall intensities. In our study, we have found an influence factor of 20 when the rainfall intensity since the beginning of the rainfall episode is between 5 and 10 mm h^{-1} (Table 6). The MSE seems more sensitive to rainfall than the La Reunion cliffs. This may be due to the different characteristics of the rock masses and to the different rockfall volume ranges (over 0.1 m^3 for our DB2, over 2 m^3 for La Reunion). Comparing the MSE and Burgundy is more difficult because the intensity intervals are very different. However if one assumes that the frequency increases linearly with the rainfall intensity, it appears that the sensibilities of both sites are near each other.

In rock slope design, the influence of water on slope stability is usually modelled by a pressure exerted by water which partially fills the joints (Hoek and Bray, 1981). This process needs that the joints to be sealed so that water level can raise. In the MSE cliff, this situation seems very improbable because the joints are sufficiently permeable to allow water to flow outside the rock mass. The authors suggest that water acts by chemical weathering including limestone dissolution and weathering of thin marly layers.

5.3 Other causes of rockfalls

It can be seen in Table 6 that the frequency of rockfalls occurring outside rainfall or freeze–thaw episodes has been estimated to 0.021 h^{-1} from DB1. These rockfalls are caused by other factors, but these factors act also during rainfall or freeze–thaw. The number of rockfalls they have caused can be determined by multiplying the last frequency by the length of the observation period. It represents 52 % of the 854 rockfalls occurred. Earthquakes are often cited as a frequent cause of rockfalls, but it does not

appear to be significant at the MSE: none of the 89 stronger earthquakes (magnitude range 1 to 4.9) occurred in the Alpine region falls in one of the rockfall dating intervals (< 20 h) of DB2. Other possible processes which can be invoked for causing the MSE rockfalls are tectonic deformations and microcracks propagation. Progressive microcracks propagation which occurs during tertiary creep (Scholz, 1968) appears to be the main cause of rockfalls occurring outside rainfall or freeze–thaw episodes. Sandersen et al. (1986) also noted that many rockfalls are not correlated with meteorological factors.

5.4 Problem of close rockfalls

When studying the rockfall frequency or the rockfall volumes from periodic surveys, the question arises of whether a rock volume has fallen in one or several events (Abellan et al., 2010). Ideally, a truly continuous survey should be required to distinguish events which are close to each other. In the more favorable periods, our method makes it possible to distinguish events which are as close as 10 mn. From the 854 rockfall scars detected between 2012 and 2015, less than 1 % have been found to result from several distinct rockfalls. Moreover, all the 214 rockfall scars which have been more precisely dated in DB2 appear as single events in both cases. It means that a rockfall is rarely followed by an adjacent one occurring in the next hours, days or weeks.

Francou (1982) and Krautblatter et al. (2009) also pointed out the storage effect which cause secondary rockfalls. In our case, as we work with fallen compartment directly detected on the rock face, we know the rupture configuration of the compartment, and we date the moment between the presence/absence of the compartment on the cliff, without considering the deposits.

5.5 Dating precision of rockfall inventories

Comparison of results obtained with DB1 and DB2 shows the necessity of a precise rockfall database to study the influence of different meteorological and physical trig-

gering processes. We show that combining TLS detection and photographic survey allows to create more precise temporal inventories and to collect a significant number of events occurring in a precise geological and climatic context. This avoids bias which often occur in data bases including rockfalls which have occurred in different sites. Interesting results could be obtained by applying this methodology to other sites in different geological and climatic conditions.

5.6 Temporal hazard prediction

It appears in Table 5 that the rockfall frequency rapidly falls down to its "base" level (i.e. rockfall frequency without rainfall or freeze–thaw) in some hours (much less than 25 h) after a rainfall episode. It also appears in Fig. 5 that the thawing periods are usually shorter than 25 h. A simple rule can be drawn from these observations: the rockfall frequency in the MSE is not influenced by the meteorological factors one day after the end of rainfall or freezing. On the other hand, one can consider that the rockfall frequency begins to increase at the beginning of rainfall and when the temperature increases during a freezing period.

Our results make it possible to propose a more precise temporal hazard prediction based on meteorological parameters. We suggest the following hazard levels, which correspond to different values of the influence factor (with respect to the frequency without rainfall or freeze–thaw):

1. low hazard: no rainfall or freeze–thaw episode in progress for at least 24 h;
2. medium hazard (influence factor > 2): cumulative rainfall since the beginning of the rainfall episode higher than 20 mm;
3. high hazard (influence factor > 5): during negative warming, or if the cumulative rainfall since the beginning of the rainfall episode is higher than 30 mm;

4. very high hazard (influence factor > 10): during thawing (defined using the freezing potential) or when the rainfall intensity since the beginning of the rainfall episode is higher than 5 mm h^{-1}.

6 Conclusions

Terrestrial laser scanner associated with photographic survey allows studying precisely the influence of meteorological factors on rockfall occurrence. Rockfalls bigger than 0.01 m^3 can be dated with a monthly precision and rockfalls bigger than 0.1 m^3 with an hourly precision (or daily precision by cloudy weather).

Rainfall or freeze–thaw appears to have caused about half of the 854 rockfalls occurred during 887 days, but these rockfalls are concentrated in short periods. These periods have been precisely defined, allowing a quantitative prediction of the rockfall hazard depending on the weather forecast. Rockfalls caused by rainfall occur over the rainfall episode without significant delay after the last rainfall of the episode. Rockfalls caused by freeze–thaw mainly occur when the air temperature increases and until the freezing potential decreases to zero. It can be inferred that rockfalls are triggered by thermal ice dilatation rather than by dilatation due to the phase transition. But they may occur only when the ice melt, because the cohesion of the ice–rock interface can be sufficient to hold the rock compartment which has been cut.

Concerning rockfall hazard, the rockfall frequency can be multiplied by an influence factor as high as 7 during freeze–thaw episodes and 26 when the mean rainfall intensity (since the beginning of the rainfall episode) is higher than 5 mm h^{-1}. Based on our results, a 4-level hazard scale has been proposed for hazard prediction.

Acknowledgements. The authors thank the Région Rhône Alpes and Fédération VOR for fundings; Météo France and P. Hyvrard for providing meteorological data; G. Kluczinsky for allowing us to take pictures from his property.

References

Abellan, A., Calvet, J., Vilaplana, J. M., and Blanchard, J.: Detection and spatial prediction of rockfalls by means of terrestrial laser scanner monitoring, Geomorphology, 119, 162–171, doi:10.1016/j.geomorph.2010.03.016, 2010.

Abellan, A., Oppikofer, T., Jaboyedoff, M., Rosser, N. J., Lim, M., and Lato, M. J.: Terrestrial laser scanning of rock slope instabilities, Earth Surf. Proc. Land., 39, 80–97, doi:10.1002/esp.3493, 2014.

Bertrand-Krajewski, J.: Cours d'hydrologie urbaine. Partie 2: La pluie, URGC-INSA, Lyon, 2007.

Bost, M.: Altération par le gel des massifs rocheux: etude expérimentale et modélisation des mécanismes de génération des contraintes dans les fissures, PhD Thesis, Ecole Nationale des Ponts et Chaussées, Paris, 2008.

Brazdil, R., Silhan, K., Panek, T., Dobrovolny, P., Kasickova, L., and Tolasz, R.: The influence of meteorological factors on rockfall in the Moracskoslezské Beskydy Mts, Geografie, 117, 1–20, 2012.

Chanut, M. A., Barthelet, V., and Kasperski, J.: Contribution de l'imagerie de face pour l'analyse des mouvements de terrain: application au versant de Séchilienne, Journées Aléas Gravitaires, Strasbourg, 2011.

Chardon, M.: Excursion géographique: la Chartreuse, Rev. Geogr. Alp., 75, 315–351, doi:10.3406/rga.1987.2687, 1987.

Chau, K. T., Wong, R. H. C., Liu, J., and Lee, C. F.: Rockfall hazard analysis for Hong Kong based on rockfall inventory, Rock Mech. Rock Eng., 36, 383–408, doi:10.1007/s00603-002-0035-z, 2003.

Cruden, D. and Varnes, D. J.: Landslides types and processes, in: Landslides: Investigation and Mitigation, vol. 247, edited by: Turner, A. K. and Schuster, R. L., Transportation Research Board, Washington, D.C., 36–75, 1996.

D'Amato, J.: Apport des bases de données d'éboulements rocheux obtenues par scanner laser dans la caractérisation des conditions de rupture et processus associés, Université Grenoble Alpes, Grenoble, 2015.

Dash, J. G., Rempel, A. W., and Wettlaufer, J. S.: The physics of premelted ice and its geophysical consequences, Rev. Mod. Phys., 78, 696–734, doi:10.1103/RevModPhys.78.695, 2006.

Davidson, G. P. and Nye, J.: A photoelastic study of ice pressure in rock cracks, Cold Reg. Sci. Technol., 11, 141–153, 1985.

Davies, M. C. R., Hamza, O., Lumsden, B. W., and Harris, C.: Laboratory measurement of the shear strength of ice-filled rock joints, Ann. Glaciol., 31, 463–467, 2000.

Delonca, A., Gunzburger, Y., and Verdel, T.: Statistical correlation between meteorological and rockfall databases, Nat. Hazards Earth Syst. Sci., 14, 1953–1964, doi:10.5194/nhess-14-1953-2014, 2014.

DeRoin, N. and McNutt, S. R.: Rockfalls at Augustine Volcano, Alaska: the influence of eruption precursors and seasonal factors on occurrence patterns 1997–2009, J. Volcanol. Geoth. Res., 211–212, 61–75, doi:10.1016/j.jvolgeores.2011.11.003, 2012.

Douglas, G. R.: Magnitude frequency study of rockfall in co. Antrim, N. Ireland., Earth Surf. Processes, 5, 123–129, 1980.

Douguédroit, A. and Saintignon, M. F.: Les gradients de températures et de précipitations en montagne, Rev. Geogr. Alp., 72, 225–240, doi:10.3406/rga.1984.2566, 1984.

Fiorio, B., Meyssonnier, J., and Boulon, M.: Experimental study of the friction of ice over concrete under simplified ice-structure interaction conditions, Can. J. Civil Eng., 29, 347–359, doi:10.1139/L02-012, 2002.

Francou, B.: Chutes de pierres et éboulisation dans les parois de l'étage périglaciaire, Rev. Geogr. Alp., 70, 279–300, doi:10.3406/rga.1982.2508, 1982.

Frayssines, M. and Hantz, D.: Failure mechanisms and triggering factors in calcareous cliffs of the Subalpine Ranges (French Alps), Eng. Geol., 86, 256–270, doi:10.1016/j.enggeo.2006.05.009, 2006.

Gidon, M.: Les décrochements et leur place dans la structuration du massif de la Chartreuse (Alpes occidentales françaises), Rev. Geogr. Alp., 66, 39–55, 1990.

Guerin, A., Hantz, D., Rossetti, J.-P., and Jaboyedoff, M.: Brief communication "Estimating rockfall frequency in a mountain limestone cliff using terrestrial laser scanner", Nat. Hazards Earth Syst. Sci. Discuss., 2, 123–135, doi:10.5194/nhessd-2-123-2014, 2014.

Gunzel, F. K.: Shear strength of ice filled rock joints, in: Proceedings of the 9th International Conference on Permafrost, Fairbanks, Alaska, USA, 2008.

Gunzel, F. K.: Shear strength of rock joints filled with frozen sand, in: Proceedings of the 10th International Conference on Permafrost (TICOP), Salekhard, Russia, 2012.

Hale, A. J., Calder, E. S., Loughlin, S. C., Wadge, C., and Ryan, G. A.: Modelling the lava dome extruded at Souffrière Hills Volcano, Montserrat, August 2005–May 2006.

Part II: Rockfall activity and talus deformation, J. Volcanol. Geoth. Res., 187, 69–84, doi:10.1016/j.jvolgeores.2009.08.014, 2009.
Hallet, B.: Why do freezing rocks break?, Science, 314, 1092–1093, doi:10.1126/science.1135200, 2006.
Hantz, D.: Quantitative assessment of diffuse rock fall hazard along a cliff foot, Nat. Hazards Earth Syst. Sci., 11, 1303–1309, doi:10.5194/nhess-11-1303-2011, 2011.
Hoek, E. and Bray, J. W.: Rock Slope Engineering, The Institution of Mining and Metallurgy, London, 1981.
Huggel, C., Clague, J. J., and Korup, O.: Is climate change responsible for changing landslide activity in high mountains?, Earth Surf. Proc. Land., 37, 77–91, doi:10.1002/esp.2223, 2012.
Jaboyedoff, M., Oppikofer, T., Abellan, A., Derron, M.-H., Loye, A., Metzger, R., and Pedrazzini, A.: Use of LiDAR in landslide investigations: a review, Nat. Hazards, 61, 5–28, doi:10.1007/s11069-010-9634-2, 2012.
Jail, M.: Recherches sur les variations thermiques le long d'un adret. Etude statistique et dynamique, Rev. Geogr. Alp., 54, 233–253, doi:10.3406/rga.1966.3257, 1966a.
Jail, M.: Température et types de temps le long d'un adret, Rev. Geogr. Alp., 54, 443–456, doi:10.3406/rga.1966.3271, 1966b.
Kobayashi, Y., Harp, E. L., and Kagawa, T.: Simulation of rockfalls triggered by earthquakes, Rock Mech. Rock Eng., 23, 1–20, 1990.
Krautblatter, M. and Moser, M.: A nonlinear model coupling rockfall and rainfall intensity based on a four year measurement in a high Alpine rock wall (Reintal, German Alps), Nat. Hazards Earth Syst. Sci., 9, 1425–1432, doi:10.5194/nhess-9-1425-2009, 2009.
Letortu, P.: Le recul des falaises crayeuses haut-normandes et les inondations par la mer en Manche centrale et orientale: de la quantification de l'aléa à la caractérisation des risques induits, PhD Thesis, Université de Caen Basse-Normandie, Caen, 13, 2012.
Luckman, B. H.: Rockfalls and rockfall inventory data: some observations from Surprise Valley, Jasper National Park, Canada, Earth Surf. Process., 1, 287–298, 1976.
Malamud, B. D., Turcotte, D. L., Guzzetti, F., and Reichenbach, P.: Landslides, earthquakes and erosion, Earth Planet. Sc. Lett., 229, 45–59, doi:10.1016/j.epsl.2004.10.018, 2004.
Mateos, R. M., Garcia-Moreno, I., and Azanon, J. M.: Freeze–thaw cycles and rainfall as triggering factors of mass movements in a warm Mediterranean region: the case of the Tramuntana Range (Majorca, Spain), Landslides, 9, 417–432, doi:10.1007/s10346-011-0290-8, 2012.

Matsuoka, N.: Diurnal freeze–thaw depth in rockwalls: field measurements and theoretical considerations, Earth Surf. Proc. Land., 19, 423–435, 1994.
Matsuoka, N.: Direct observations of frost wedging in alpine bedrock, Earth Surf. Proc. Land., 26, 601–614, 2001.
Matsuoka, N. and Sakai, H.: Rockfall activity from an alpine cliff during thawing periods, Geomorphology, 28, 309–328, 1999.
MELTT – Ministère de l'Equipement, du Logement, des Transports et du Tourisme: Tangentielle Est–Ouest Agglomération Grenobloise. Etude de génie civil et d'environnement des tunnels et tranchées, Phase 1: Analyse des problèmes et de la situation actuelle, Grenoble, 1997.
Montagnat, M., Weiss, J., Cinquin-Lapierre, B., Labory, P. A., Moreau, L., Damilano, F., and Lavigne, D.: Waterfall ice: formation, structure, and evolution, J. Glaciol., 56, 225–234, 2010.
Murton, J. B., Peterson, R., and Ozouf, J.-C.: Bedrock fracture by ice segregation in cold regions, Science, 314, 1127–1129, doi:10.1126/science.1132127, 2006.
Optech: ILRIS-LR Terrestrial Laser Scanner, Summary Specification Sheet, available at: http://www.teledyneoptech.com/wp-content/uploads/ILRIS-LR-Spec-Sheet-140730-WEB.pdf, last access: 11 December 2015.
Perret, S., Stoffel, M., and Kienholz, H.: Spatial and temporal rockfall activity in a forest stand in the Swiss Prealps – a dendrogeomorphological case study, Geomorphology, 74, 219–231, doi:10.1016/j.geomorph.2005.08.009, 2006.
Rakotomalala, R.: Econométrie: La régression linéaire simple et multiple, http://eric.univ-lyon2.fr/~ricco/publications.html, last access: 11 December 2015.
Ravanel, L.: Caractérisation, facteurs et dynamiques des écroulements rocheux dans les parois à permafrost du massif du Mont Blanc, PhD Thesis, Université de Savoie, Chambéry, 2010.
Rosser, N. J., Petley, D., Lim, M., Dunning, S. A., and Allison, R. J.: Terrestrial laser scanning for monitoring the process of hard rock coastal cliff erosion, Q. J. Eng. Geol. Hydroge., 28, 363–375, 2005.
Sandersen, F., Bakkehoi, S., Hestnes, E., and Lied, K.: The influence of meteorological factors on the initiation of debris flows, rockfalls, rockslides and rockmass stability, edited by: Senneset, K., Balkema, Rotterdam, 1996.
Sass, O. and Oberlechner, M.: Is climate change causing increased rockfall frequency in Austria?, Nat. Hazards Earth Syst. Sci., 12, 3209–3216, doi:10.5194/nhess-12-3209-2012, 2012.
Scholz, C.: Mechanism of creep in brittle rock, J. Geophys. Res., 73, 3295–3302, 1968.

Tharp, T. M.: Conditions for crack propagation by frost wedging, Geol. Soc. Am. Bull., 99, 94–102, 1987.
Viles, H. A.: Linking weathering and rock slope instability: non-linear perspectives, Earth Surf. Proc. Land., 38, 62–70, doi:10.1002/esp.3294, 2013.
Walder, J. and Hallet, B.: A theoritical model of the fracture of rock during freezing, Geol. Soc. Am. Bull., 96, 336–346, 1985.
Wei, L.-W., Chen, H., Lee, C.-F., Huang, W.-K., Lin, M.-L., Chi, C.-C., and Lin, H.-H.: The mechanism of rockfall disaster: a case study from Badouzih, Keelung, in northern Taiwan, Eng. Geol., 183, 116–126, doi:10.1016/j.enggeo.2014.10.008, 2014.
Yamagishi, H.: Recent landslides in western Hokkaido, Japan, Pure Appl. Geophys., 157, 1115–1134, 2000.
Yin, Y., Wang, F., and Sun, P.: Landslide hazards triggered by the 2008 Wenchuan earthquake, Sichuan, China, Landslides, 6, 139–151, doi:10.1007/s10346-009-0148-5, 2009.

Table 1. Meteorological factors and triggering mechanisms.

Weather event	Processes proposed for rockfall triggering	Relevant meteorological parameters
Rainfall (intense or prolonged)	Water pressure in rock joint	Intensity ($mm\,h^{-1}$), amount (mm)
	Clay swelling in rock joint Dissolution (chemical action) Leaching (mechanical action)	Duration (h)
Freeze–thaw	Ice frost wedging: ice pressure due ice formation (confined dilatation) + sealing of cracks leading to water pressure	Negative temperature (°C), negative gradient ($°C\,h^{-1}$)
	Ice thermal wedging: ice pressure due to confined thermal dilatation	Negative temperature (°C), positive gradient ($°C\,h^{-1}$)
	Ice melting: loss of cohesion	Positive temperature (°C)
Snow and ice melt	Water pressure in rock joint	Positive temperature (°C) and gradient ($°C\,h^{-1}$), solar radiation ($W\,m^{-2}$)
Sunshine	Thermal stresses which propagate cracks	Temperature (°C), solar radiation ($W\,m^{-2}$)

Table 2. Studies of the influence of meteorological factors on rockfall occurrence.

Author	Country	Elevation (m a.s.l.)	Geology	Detection method	Duration (years)	Nb of RF	Dating precision	Volume range (m^3)*	Results on influence of meteorological factors
Luckman (1976)	Canada	1800–2500	sandy and calcareous limestone	direct observation, deposit observations	8	239	Hour or more		Diurnal occurrence of rockfall. RF activity: max in spring and during storms in the summer
Douglas (1980)	Ireland	0–100	basalt	collection of rock debris on square or in a box	4		Week	0,0004–0,002 (*T*)	Correlation between nb of freeze–thaw event and RF, and % of period below 0 °C and RF.
Sandersen et al. (1986)	Norway	0–2400	crystalline rocks	newspaper report	1	91	Day	< 1000	Continental climate: higher activity during snowmelt season; marine climate: higher activity during autumn. Many RF not correlated with weather factors
Matsuoka and Sakai (1999)	Japan	2800–3200	sandstone and shale	rock debris on snow	14			0–18 (*A*)	Max RF activity: about 10 days after meltout (seasonal thawing). No correlation with precipitation or diurnal frost cycles.
Chau et al. (2003)	Hong Kong	0–957	Volcanic and granitic rocks	deposit on human infrastructures	15	368		1–1000 (*E*)	Influence of rainfall, lower threshold of daily rainfall 150–200 mm
Frayssines and Hantz (2006)	France (Subalpine Ranges)	200–2000	limestone	historical inventory	34	46	Day	10–30 × 10^3 (*E*)	Influence of freeze–thaw cycles, slight influence of rainfall and no influence of earthquakes
Perret et al. (2006)	Switzerland	1200–1700	limestone	dendrogeomorphic dating	121	250	Season		Rockfall activity increased over last century. Seasonnal occurrence of RF: early spring. Positive correlation with temperature. No correlation with precipitations
Ravanel (2010)	France (Mont Blanc Massif)	2600–3700 2200–4200	granite	old photographs, direct observations and TLS	150 4	50 321	Decade to Day	350–265 × 10^3 (*E*) 0.1–50 × 10^3 (*E*)	Influence of permafrost retreat and loss of glacier buttressing
Sass and Oberlechner (2012)	Austria	300–2700 +	?	historical inventory	102	252	Year	< 10^6 (*E*)	No increase of RF frequency below permafrost due to global warming
Brazdil et al. (2012)	Czech Republic	600–970	sandstone, claystone, mudstone	dendrogeomorphic dating	78 max	989	Year	< 5 m^3 (*B*)	No conclusion on the influence of climatic factors (bias in the Rockfall Rate time series)
Mateos et al., (2012)	Majorca Island	200–700	limestone and dolostone	deposits on roads	2	14	Day	2–300 × 10^3 (*E*)	Influence of intense rainfall > 90 mm (24 h^{-1}). Influence of antecedent rainfall over 800 mm, and freeze–thaw cycles.
Letortu (2013)	France (Normandie Coast)	0–200	limestone	deposit observation + historical inventory	7	331	Week	1–236 × 10^3 (*E*)	Influence of effective precipitations, then freeze–thaw cycles. Sea agitation and tide coefficients can have effects.
Delonca et al. (2014)	France (Réunion, Burgundy, Auvergne)	0–200 300–400 700–900	basalt, limestone, granite	deposit on french railway network	0,3 to 1,4	949 135 142	Day	2–27 × 10^3 (*E*) 8–8 × 10^3 (*E*) 2–6 × 10^3 (*E*)	Réunion: correlation with rainfall. Burgundy: correlation with rainfall. Auvergne: correlation with daily minimum temperature
This paper	France (Subalpine Ranges)	800–1300	thinly bedded limestones	TLS + photographic survey of scars	2.4	854	10 min to month	0.001–1500 (*E*)	Highest rockfall frequency during freeze–thaw episodes, especially during thawing periods. Secondary influence of rainfall.

E: volume of event.
B: volume of individual block.
T: total volume on period.
Y: yearly volume.

Table 3. Technical information of rockfall databases.

Data base	Camera type	Lens focale distance	Sensor size	Approximate pixel size	Photo precision	Minimal detected volume (m^3)	Photo interval	Datation precision	Number of rockfalls	Number of days
DB 1	Nikon 50D	300 mm	6 Mpx	3 cm real	High	0.002	Month	Low	854	887
DB 2	Canon EOS Rebel T3 1100D	24 mm	12 Mpx	21 cm real	Low	0.04	10 mn	High	214	810

Table 4. Multiple linear regression values, considering rainfall and freeze–thaw, and rainfall and thaw only.

1) Rainfall and Freeze–thaw vs. rockfall frequency						
DURATION						
Multiple regression						
R^2	0.47					
R^2 adjusted	0.42					
Multiple regression coefficients:				Standardized regression coefficients:		
	Rftd	Rrd	constant		$Rftd_{st}$	Rrd_{st}
b	0.068	0.022	0.022	β	0.71	0.10
σb	0.016	0.037	0.010	$\sigma\beta$	0.16	0.16
AMOUNT						
Multiple regression						
R^2	0.48					
R^2 adjusted	0.43					
Multiple regression coefficients:				Standardized regression coefficients:		
	Rfta	Rra	constant		$Rfta_{st}$	Rra_{st}
b	0.030	0.059	0.020	β	0.71	0.15
σb	0.007	0.064	0.010	$\sigma\beta$	0.16	0.16
2) Rainfall and Thaw vs. rockfall frequency						
DURATION						
Multiple regression						
R^2	0.51					
R^2 adjusted	0.46					
Multiple regression coefficients:				Standardized regression coefficients:		
	Rtd	Rrd	constant		Rtd_{st}	Rrd_{st}
b	0.181	0.018	0.023	β	0.73	0.08
σb	0.039	0.035	0.010	$\sigma\beta$	0.16	0.16
AMOUNT						
Multiple regression						
R^2	0.51					
R^2 adjusted	0.47					
Multiple regression coefficients:				Standardized regression coefficients:		
	Rta	Rra	constant		Rta_{st}	Rra_{st}
b	0.071	−0.003	0.027	β	0.72	−0.01
σb	0.015	0.060	0.009	$\sigma\beta$	0.15	0.15

Table 5. "Certain" and "statistical" rockfall frequencies based on the DB2 for different meteorological conditions.

		Certain frequency		Statistical frequency	
	Duration (h)	Number of rockfalls	Rockfall frequency (h^{-1})	Number of rockfalls	Rockfall frequency (h^{-1})
Complete period	19 440	98	0.0050	144	0.0074
Rainfall episods	4282	51	0.0119	62	0.0145
within 24 h after rainfall	3288	9	0.0027	21	0.0064
24 to 48 h after rainfall	3288	8	0.0024	19	0.0058
48 to 72 h after rainfall	3288	2	0.0006	8	0.0024
Freeze–thaw episodes	2084	14	0.0067	25	0.0120
No meteorological factor	3243	14	0.0043	18	0.0056
Rainfall and freeze–thaw	221	0	0.0000	1	0.0045
Negative cooling periods	846	2	0.0024	8	0.0095
Negative warming periods	374	2	0.0053	5	0.0134
Thawing periods	864	10	0.0116	12	0.0139

Table 6. Influence factors for different situations. Factor 1 is related to the mean frequency of rockfalls. Factor 2 is related to the frequency without rainfall or freeze–thaw.

Approach Data base	Statistical DB1	Statistical DB2	Certain DB2
Volume range (m^3)	$0.01–10^3$	$0.1–10^3$	$0.1–10^3$
Rockfall number	854	144	98
Mean frequency (h^{-1})	0.04	0.0074	0.005
Frequency without rainfall or freeze–thaw (h^{-1})	0.021	0.0056	0.0043
Frequency during freeze–thaw (h^{-1})	0.147	bias	bias
Freeze–thaw factor 1	3.7	bias	bias
Freeze–thaw factor 2	7.0	bias	bias
Frequency during rainfall (h^{-1})	bias	0.0145	0.0119
Rainfall factor 1	bias	2.0	2.4
Rainfall factor 2	bias	2.6	2.8
Mean frequency for periods without freeze–thaw (h^{-1})	0.022		
Frequency without rainfall for periods without freeze–thaw (h^{-1})	0.012		
Frequency during rainfall for periods without freeze–thaw (h^{-1})	0.054		
Rainfall factor 1	2.5		
Rainfall factor 2	4.5		
Frequency for mean rainfall intensity > 5 mm h^{-1}		0.15	
Rainfall factor 1		20.3	
Rainfall factor 2		26.8	

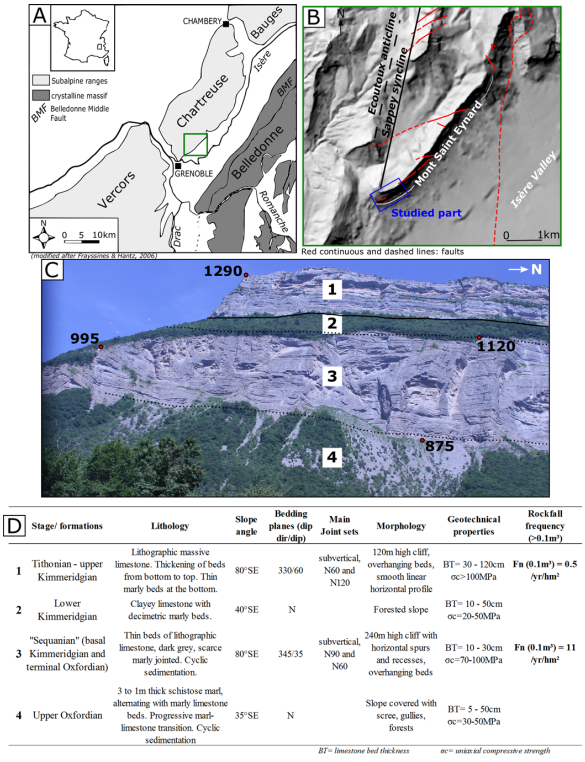

D

	Stage/ formations	Lithology	Slope angle	Bedding planes (dip dir/dip)	Main Joint sets	Morphology	Geotechnical properties	Rockfall frequency (>0.1m³)
1	Tithonian - upper Kimmeridgian	Lithographic massive limestone. Thickening of beds from bottom to top. Thin marly beds at the bottom.	80°SE	330/60	subvertical, N60 and N120	120m high cliff, overhanging beds, smooth linear horizontal profile	BT= 30 - 120cm σc>100MPa	**Fn (0.1m³) = 0.5 /yr/hm²**
2	Lower Kimmeridgian	Clayey limestone with decimetric marly beds.	40°SE	N		Forested slope	BT= 10 - 50cm σc=20-50MPa	
3	"Sequanian" (basal Kimmeridgian and terminal Oxfordian)	Thin beds of lithographic limestone, dark grey, scarce marly jointed. Cyclic sedimentation.	80°SE	345/35	subvertical, N90 and N60	240m high cliff with horizontal spurs and recesses, overhanging beds	BT= 10 - 30cm σc=70-100MPa	**Fn (0.1m³) = 11 /yr/hm²**
4	Upper Oxfordian	3 to 1m thick schistose marl, alternating with marly limestone beds. Progressive marl-limestone transition. Cyclic sedimentation	35°SE	N		Slope covered with scree, gullies, forests	BT= 5 - 50cm σc=30-50MPa	

BT= limestone bed thickness *σc= uniaxial compressive strength*

Figure 1. (a) Simplified geological map of the Subalpine Ranges. **(b)** DEM of the studied zone, with structural features. **(c)** Photograph of the studied part of the Mont Saint Eynard. Dashed lines: supposed geological limit; continuous line: confirmed geological limit. **(d)** Geological and geotechnical information (Chardon, 1987; MELTT, 1997).

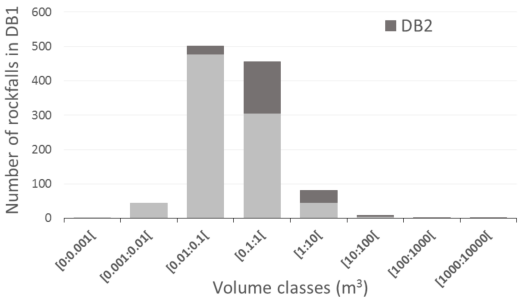

Figure 2. Volume distribution of the two databases.

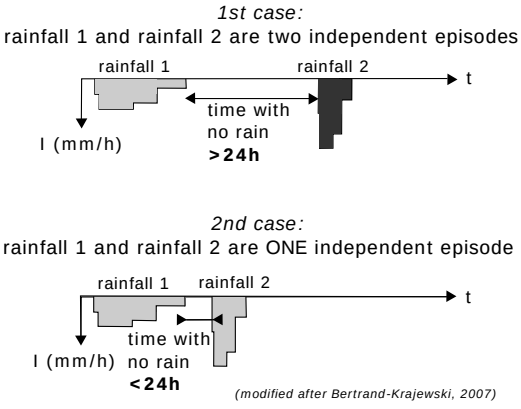

Figure 3. Schematic representation of the definition of an independent rainfall episode.

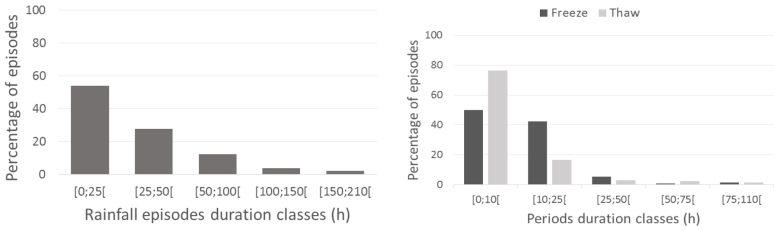

Figure 4. Distribution of rainfall episodes duration, and freezing and thawing periods duration. More than 80 % of thawing episodes are shorter than 12 h, and almost 95 % of thawing periods are shorter than 24 h. Long thawing periods occurred only at the end of the winter, when no freeze occurs anymore.

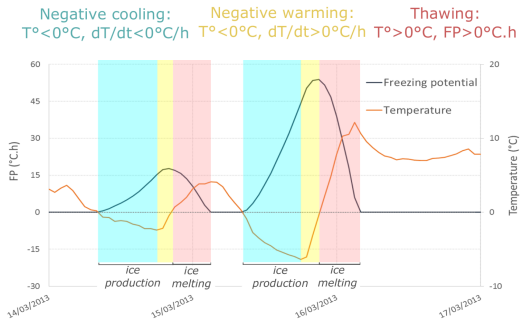

Figure 5. Definition of the three types of period within a freeze–thaw episode.

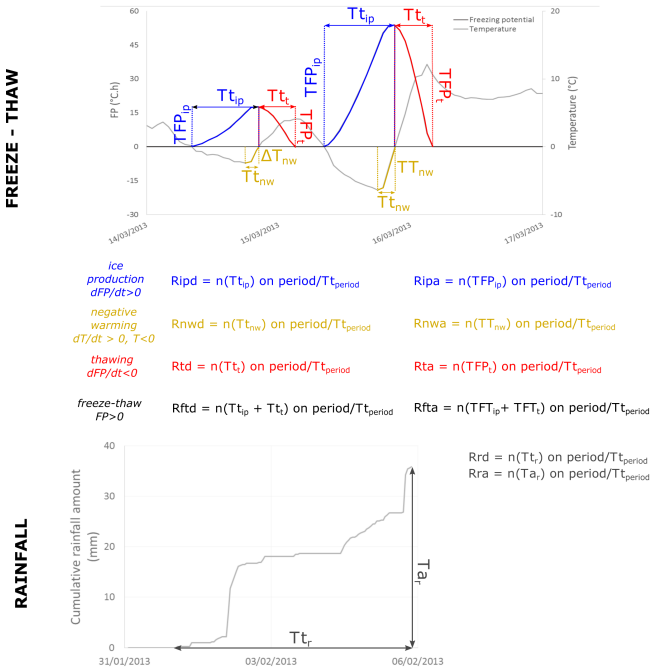

Figure 6. Description of ratios used to quantify freeze–thaw and rainfall amount and duration for each dating period of the DB1. These ratios are used for the multiple linear regression.

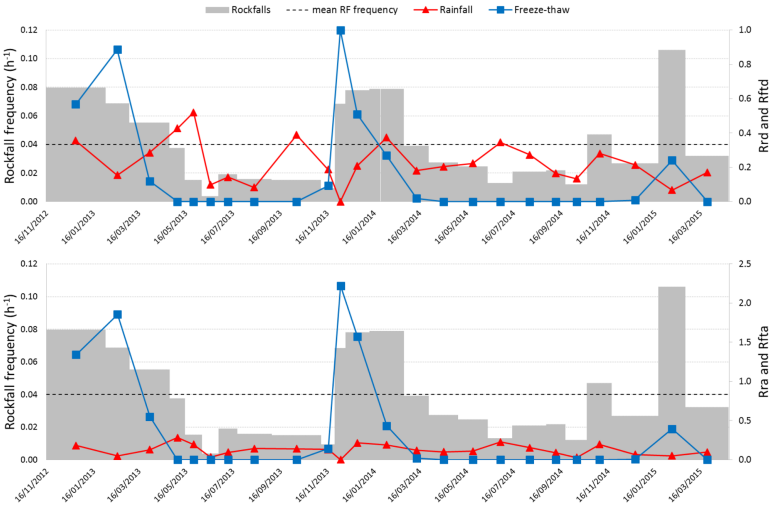

Figure 7. Rockfall frequency for the different observation periods, with rainfall and freeze–thaw duration ratios (upper panel) or rainfall and freeze–thaw amount ratios (lower panel).

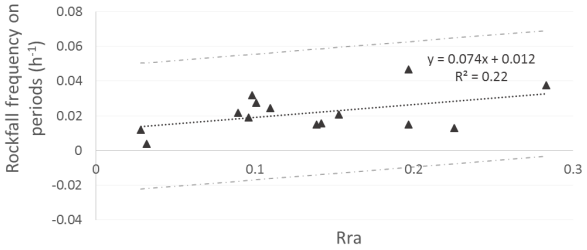

Figure 8. Simple linear regression between rainfall amount ratio (Rra) and rockfall frequency for dating periods without freeze–thaw. Dashed grey lines: 95 % interval confidence.

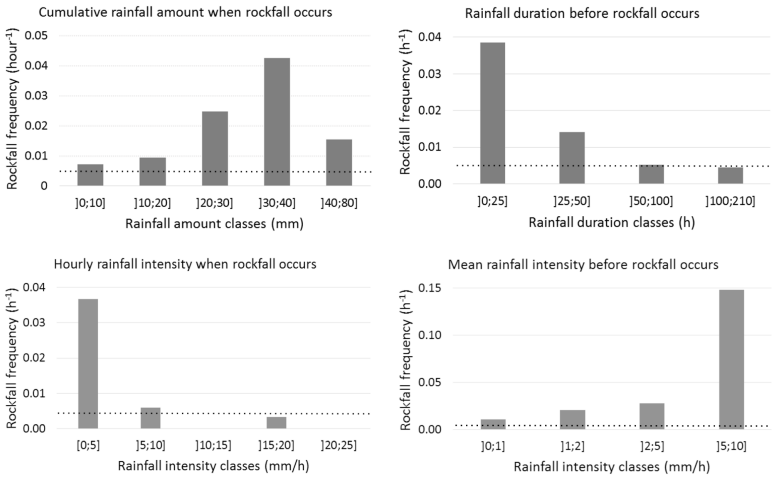

Figure 9. Rockfall frequency for different rainfall amount, rainfall duration and rainfall intensity. Dashed black lines show rockfall frequency without meteorological perturbations.

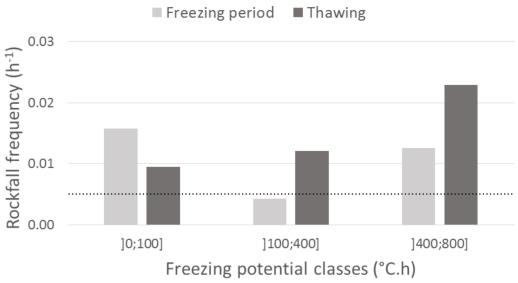

Figure 10. Rockfall frequency according to the freezing potential for freezing periods and thawing periods.

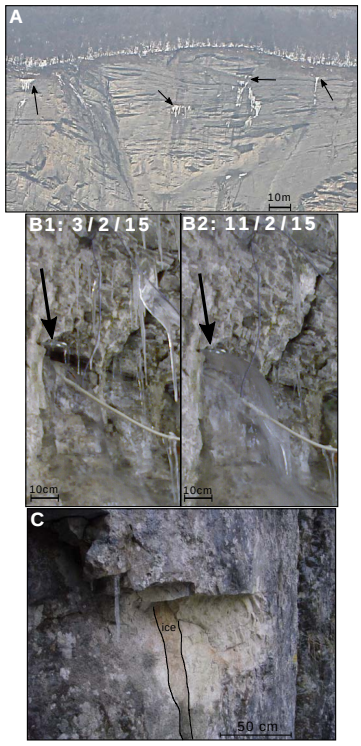

Figure 11. (a) MSE at the beginning of a thawing period. Ice formed by water coming from the forested ledge or from joints is still visible (black arrows). **(b)** Photographic survey of a crack in the Vercors Massif. **(b1)** The crack is still open. **(b2)** The crack is totally filled with ice. **(c)** Ice slab on a rockfall scar (Vercors Massif).